



RESEARCH ARTICLE

Structure and crystallization behavior of complex mold flux glasses in the system CaO-Na₂O-Li₂O-CaF₂-B₂O₃-SiO₂: A multi-nuclear NMR spectroscopic study

Tae-min Yeo^{1,4}  | Jung-Wook Cho^{1,2}  | Ivan Hung³ | Zhehong Gan³ | Sabyasachi Sen⁴ 

¹Graduate Institute of Ferrous & Energy Materials Technology, Pohang University of Science and Technology (POSTECH), Pohang, Republic of Korea

²Division of Advanced Nuclear Engineering (DANE), Pohang University of Science and Technology (POSTECH), Pohang, Republic of Korea

³National High Magnetic Field Laboratory, Tallahassee, Florida, USA

⁴Department of Materials Science and Engineering, University of California at Davis, Davis, California, USA

Correspondence

J.-W. Cho, Graduate Institute of Ferrous & Energy Materials Technology, Pohang University of Science and Technology (POSTECH), Pohang, 37673, Republic of Korea.

Email: jungwook@postech.ac.kr

S. Sen, Department of Materials Science and Engineering, University of California at Davis, Davis, CA 95616, USA.

Email: sbsen@ucdavis.edu

Funding information

Korea Institute for Advancement of Technology (KIAT); Korea Government (MOTIE), Grant/Award Number: P0017304; Human Resource Development Program for Industrial Innovation; POSCO Research Laboratory, Pohang, Korea, Industrial Strategic Technology Development Program, Grant/Award Number: 10063056; Ministry of Trade, Industry & Energy (MOTIE), Korea; National Science Foundation (NSF), Grant/Award Number: DMR-1855176

Abstract

The structure of mold flux glasses in the system CaO-(Na,Li)₂O-SiO₂-CaF₂ with unusually high modifier contents, stabilized by the addition of ~4 mol% B₂O₃, is studied using ⁷Li, ²³Na, ¹⁹F, ¹¹B, and ²⁹Si magic-angle-spinning (MAS), and ⁷Li{¹⁹F} and ²³Na{¹⁹F} rotational echo double-resonance (REDOR) nuclear magnetic resonance (NMR) spectroscopy. When taken together, the spectroscopic results indicate that the structure of these glasses consists primarily of dimeric [Si₂O₇]⁻⁶ units that are linked to the (Ca,Na,Li)-O coordination polyhedra, and are interspersed with chains of corner-shared BO₃ units. The F atoms in the structure are exclusively bonded to Ca atoms, forming Ca(O,F)_n coordination polyhedra. This structural scenario is shown to be consistent with the crystallization of cuspidine (3CaO·2SiO₂·CaF₂) from the parent melts on slow supercooling. The progressive addition of Li to a Na-containing base composition results in a corresponding increase in the undercooling required for the nucleation of cuspidine in the melt, which is attributed to the frustrated local structure caused by the mixing of alkali ions.

KEYWORDS

crystallization, cuspidine, glass, mold flux, NMR spectroscopy, structure

1 | INTRODUCTION

The development of novel mold fluxes has been an active area of investigation to improve the productivity and quality of steel products. Mold fluxes play a significant role in the continuous casting process, controlling heat transfer and lubrication between the solidified

steel shells, and the water-cooled copper mold.^{1,2} These fluxes are multi-component glass-forming liquids predominantly based on the ternary system CaO-SiO₂-CaF₂, with additives such as B₂O₃, Al₂O₃ and various alkali oxides that are used according to the specific needs of the system.³ In particular, the addition of alkali oxides enhances the crystallization of cuspidine (3CaO·2SiO₂·CaF₂) from these

liquids by lowering the activation energy of crystal growth that could be linked to a concomitant lowering of the viscosity.^{4–8} Moreover, an increase in the concentration of CaO:SiO₂ ratio^{5,9,10} or that of an alkali oxide such as Na₂O^{11,12} has been shown to increase the crystallization temperature of cuspidine. This accelerated crystallization kinetics can be related to a lowering of the viscosity of the liquid resulting from a progressive depolymerization of the silicate network. However, recent studies reported that the addition of Li₂O to CaO-Na₂O-SiO₂-CaF₂ based melts delayed both isothermal and non-isothermal melt-crystallization of cuspidine that is, crystallization occurred at greater undercoolings.¹³ A number of studies have hypothesized that the Li ions selectively form Li-F bonds in the glass structure,^{14,15} or bonds with the non-bridging oxygen (NBO) in silicates,^{13,16,17} and consequently lower the activity of F and NBO, which led to the crystallization delay. However, the structure of these glasses/liquids and its role on the crystallization of cuspidine remain poorly understood to date. It is to be noted that the structure of cuspidine can be described as consisting of ribbons of edge-sharing Ca(O,F)₆ octahedra that are interspersed by and cross-linked with dimeric Si₂O₇ groups via sharing of vertices forming Si-O-Ca linkages. In this structure the F atoms are bonded only to Ca.^{18,19}

CaO-R₂O-SiO₂-CaF₂ (R = Na, Li) based mold fluxes with high basicity (CaO/SiO₂ > 1.3) are expected to produce the appropriate crystallization kinetics of cuspidine crystals to be industrially useful.^{20,21} The purpose of the present study is to investigate the connection between the atomic structure and the crystallization of cuspidine in such highly modified network liquids in the system CaO-SiO₂-CaF₂, as well as the role of Li₂O addition on the kinetics of crystallization. However, these liquids are rather poor glass-formers due to their instability against crystallization, which precludes the possibility of their structural studies in the glassy state. Therefore, in the present study a small amount of B₂O₃ (~ 4 mol%) is incorporated in order to facilitate glass formation and thus, to enable structural analysis of the derived glasses. To this end, we have utilized multi-nuclear (⁷Li, ²³Na, ¹⁹F, ²⁹Si, ¹¹B) magic-angle-spinning (MAS) and ⁷Li{¹⁹F} and ²³Na{¹⁹F} rotational echo double-resonance (REDOR) nuclear magnetic resonance (NMR) spectroscopy to elucidate the nature of the short-range order and the modifier-fluorine interaction in the structure of these glasses.

2 | EXPERIMENTAL PROCEDURE

2.1 | Sample preparation

Three CaO-Na₂O-SiO₂-CaF₂-B₂O₃ glass samples with 0, 2, and 4 mol% Li₂O (denoted henceforth as L0, L2, and

TABLE 1 Analyzed chemical composition in mol% of glasses investigated in this study

Oxide	Glass code		
	L0	L2	L4
Li ₂ O	0.00	2.20	4.25
CaF ₂	18.27	18.62	18.07
SiO ₂	31.23	30.61	29.95
CaO	38.60	36.79	36.14
Na ₂ O	7.55	7.34	7.22
B ₂ O ₃	4.36	4.45	4.37

L4, respectively) were synthesized using reagent-grade Li₂CO₃, SiO₂, CaCO₃, Na₂CO₃, CaF₂, and B₂O₃. The compositions of all glasses were designed to keep the Ca:Si molar ratio fixed at ~1.8. These reagents were mixed for two hours and melted in amorphous carbon crucibles in a box furnace at 1573 K for 30 min. The melts were quenched on a cold copper plate to obtain the corresponding glasses. The resulting samples were ground by disk milling and chemically analyzed via X-ray fluorescence (XRF) and inductively coupled plasma—atomic emission spectrometry (ICP-AES). The analyzed chemical compositions in mol% for all glasses are reported in Table 1 and in wt% in Table S1.

2.2 | Calorimetric analysis

The crystallization behavior of these glass-forming liquids was investigated using differential scanning calorimetry (DSC, Netzsch STA 449C; Netzsch Instrument Inc., Germany). For each glass composition approximately 50 mg of crushed glass sample was placed in a platinum crucible (5 mm diameter and 5 mm height), and was held for 5 min at an initial temperature of 323 K. The sample was subsequently heated at 10 K/min to 1573 K, where it was held for 5 min for homogenization and fining. Finally, the sample was cooled at a constant rate of 10 K/min from 1573 K to room temperature. The liquidus temperature T_m was taken at the endothermic peak obtained at a heating rate of 10 K/min. The crystallization temperature T_c of cuspidine was determined by the onset temperature of exothermic curve obtained at a cooling rate of 10 K/min.

2.3 | X-ray diffraction

Since the sample volume used in DSC measurements was too small to perform powder X-ray diffraction (PXRD) for the identification of any crystal phases, heat treatment

was carried out on larger samples in a box furnace. Approximately 10 g of each sample was placed in a carbon crucible (Height: 70 mm, Inner diameter: 15 mm, Outer diameter: 20 mm). The overall heat treatment schedule was the same as the DSC heat treatment, except the samples were held isothermally at the respective crystallization temperatures for 3 hours to obtain full crystallinity. The crystalline samples thus obtained were ground and PXRD patterns were obtained using an X-ray diffractometer (Bruker AXS D8 Advance). The lack of Bragg peaks in the PXRD patterns of the glass samples confirms their amorphous nature (Figure S1).

2.4 | Multi-nuclear NMR spectroscopy

The ^7Li , ^{23}Na , and ^{19}F magic-angle spinning (MAS) NMR spectra were collected at the National High Magnetic Field Laboratory in Tallahassee, Florida, using a Bruker Avance III spectrometer and a 2.5 mm Bruker triple-resonance MAS probe operating at resonance frequencies of 470.6, 194.4, and 132.3 MHz (magnetic field 11.7 T) for ^{19}F , ^7Li , and ^{23}Na , respectively. Crushed glass samples were packed into 2.5 mm ZrO_2 rotors and spun at a MAS frequency of 18.8 kHz. The 1D ^{19}F , ^7Li , and ^{23}Na MAS NMR spectra were acquired using pulse lengths of 2.5, 20, and 10 μs (all correspond to 90° tip angle); radiofrequency (RF) fields of 100, 12.5, and 12.5 kHz; recycle delays of 40, 68, and 3 s; and 16, 32, and 256 transients, respectively. The $^7\text{Li}\{^{19}\text{F}\}$ and $^{23}\text{Na}\{^{19}\text{F}\}$ R^3 -REDOR²² NMR data were collected by application of rotary resonance recoupling (R^3) to the non-observed ^{19}F channel at the $n = 2 \text{R}^3$ condition, that is, with an RF field equal to two times the MAS frequency. The application of R^3 for heteronuclear dipolar recoupling has been shown to improve the robustness of REDOR to MAS instability. Signals acquired with (S) and without (S_0) dipolar recoupling pulses are used to obtain a REDOR fraction $\Delta S/S_0 = (S_0 - S)/S_0$ as a function of the recoupling duration,²³ which can be used to extract the heteronuclear dipolar coupling (d_{jk}) between the nuclei of interest. For an isolated pair of spins, the $\Delta S/S_0$ buildup for the original REDOR experiment can be modeled using the analytical expression,²⁴

$$\frac{\Delta S}{S_0} = (1 - x) \left[1 - \frac{\sqrt{2}\pi}{4} J_{+\frac{1}{4}} \left(\sqrt{2}d_{jk}t_{\text{mix}} \right) J_{-\frac{1}{4}} \left(\sqrt{2}d_{jk}t_{\text{mix}} \right) \right] \quad (1)$$

where J_k are Bessel functions of the first kind, and t_{mix} is the total dipolar recoupling/dephasing duration. The $(1 - x)$ term allows one to account for all factors that leave signals unperturbed by dipolar recoupling. For the R^3 -REDOR experiment, Equation (1) needs to be modified as follows:²²

TABLE 2 Crystallization (T_c) and liquidus (T_m) temperatures and undercooling (ΔT) for different samples

Sample	T_c (K)	T_m (K)	ΔT (Undercooling)
L0	1281	1512	231
L2	1189	1483	294
L4	1123	1473	350

$$\frac{\Delta S}{S_0} = (1 - x) \left[1 - \frac{\sqrt{2}\pi}{4} J_{+\frac{1}{4}} \left(\frac{\sqrt{2}\pi}{4} d_{jk}t_{\text{mix}} \right) J_{-\frac{1}{4}} \left(\frac{\sqrt{2}\pi}{4} d_{jk}t_{\text{mix}} \right) \right] \quad (2)$$

to account for the slower dephasing caused by the smaller $n = 2 \text{R}^3$ recoupling compared to a pair of π -pulses per rotor period in order not to reintroduce the homonuclear dipolar interactions among the ^{19}F .

The ^{11}B (^{29}Si) MAS NMR spectra of these glasses were collected at UC Davis using a Bruker Avance spectrometer operating at a resonance frequency of 160.5 (99.4) MHz and a 4 mm (7 mm) Bruker CPMAS probe. Samples were taken in ZrO_2 rotors and were spun at a rate of 12 kHz (7 kHz) for ^{11}B (^{29}Si) NMR. The ^{11}B MAS NMR spectra were acquired using a solids 15° pulse, a recycle delay of 0.5 s, and 5000 transients were averaged and Fourier-transformed to obtain each spectrum. On the other hand, the ^{29}Si MAS NMR spectra were collected using a 60° pulse, a recycle delay of 100 s, and 850 transients were averaged to obtain each spectrum. All NMR spectra were externally referenced by recording the naturally abundant ^{17}O signal of D_2O and using the appropriate frequency ratios reported in the IUPAC recommendations.²⁵ We have carefully checked this referencing procedure against the conventional NMR standards for all nuclides and found it to be completely consistent.

3 | RESULTS AND DISCUSSION

3.1 | Melt-crystallization of mold flux glasses

The DSC scans of samples with different Li_2O contents are shown in Figure 1A, where the exothermic peaks indicate the crystallization event during cooling from $T > T_m$, that is, melt-crystallization. The major peak in each DSC curve corresponds to the crystallization of the cuspidine ($3\text{CaO} \cdot 2\text{SiO}_2 \cdot \text{CaF}_2$) phase as evidenced by the XRD patterns (Figure 1B). Li_2O addition decreases the melt-crystallization temperature (T_c) and thus increases the degree of undercooling $\Delta T = T_m - T_c$, where T_m is the liquidus temperature (Table 2). These results clearly indicate that the crystallization of cuspidine from the melt is progressively “retarded” that is, ΔT increases upon increasing addition of Li_2O . Detailed kinetic analyses of

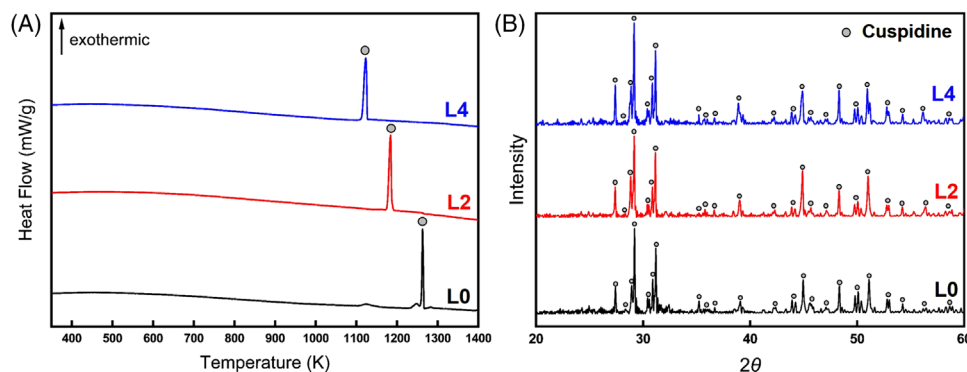


FIGURE 1 (A) DSC scans of melt-crystallization of L0, L2, and L4 compositions. The position of the exothermic peak for cuspidine crystallization is denoted with grey circle in each scan. (B) XRD patterns of melt-crystallized L0, L2, and L4 samples at respective crystallization temperatures. Black circles denote locations and relative intensities of the Bragg peaks for cuspidine (JCPDS card # 13–410)

the melt-crystallization were elucidated in our previous studies.^{14,26}

3.2 | Structural analyses with NMR spectroscopy

The ^7Li MAS NMR spectra of these glasses (Figure 2A) are characterized by a single peak centered at ~ 0.2 ppm. This chemical shift is characteristic of Li ions bonded to oxygen in silicate glasses.²⁷ It may be noted that these spectra have significant intensity near the isotropic chemical shift of -1 ppm, characteristic of LiF. Therefore, some possible association of Li with F in the structure of these glasses cannot be completely ruled out solely on the basis of these ^7Li NMR spectra. The ^{23}Na spectra of the L0, L2, and L4 glasses (Figure 2B) are characterized by a single resonance with a peak at -6.2 ppm. These ^{23}Na NMR peak positions are

typical of Na ions in silicate glasses with Na-O coordination numbers between 5 and 6.²⁸

The $^7\text{Li}\{^{19}\text{F}\}$ and $^{23}\text{Na}\{^{19}\text{F}\}$ REDOR NMR experiments (Figure 3) were carried out to determine whether there are significant bonding interactions between the Li/Na and F in the glass structure. It may be noted here that compared to the $^{23}\text{Na}\{^{19}\text{F}\}$ REDOR experiment, fewer REDOR points were collected for the $^7\text{Li}\{^{19}\text{F}\}$ experiment (Figure 3) as the ^7Li spin-lattice relaxation time T_1 was significantly longer than that of ^{23}Na , which significantly increased the data collection time for the latter. The long T_1 of ^7Li is also likely responsible for the first REDOR data point in the $^7\text{Li}\{^{19}\text{F}\}$ experiment not reaching the steady state, resulting in the observed deviation from the theoretical curve. Fitting of the $^7\text{Li}\{^{19}\text{F}\}$ REDOR buildup curve (Figure 3A) using Equation (2) gives $d_{jk} \sim 3.3$ kHz, which corresponds to a Li-F spin-pair distance of 2.4 Å. This distance is much longer than a typical Li-F bond of 1.6 ± 0.1 Å, indicating no direct bonding between lithium and fluorine in the glass

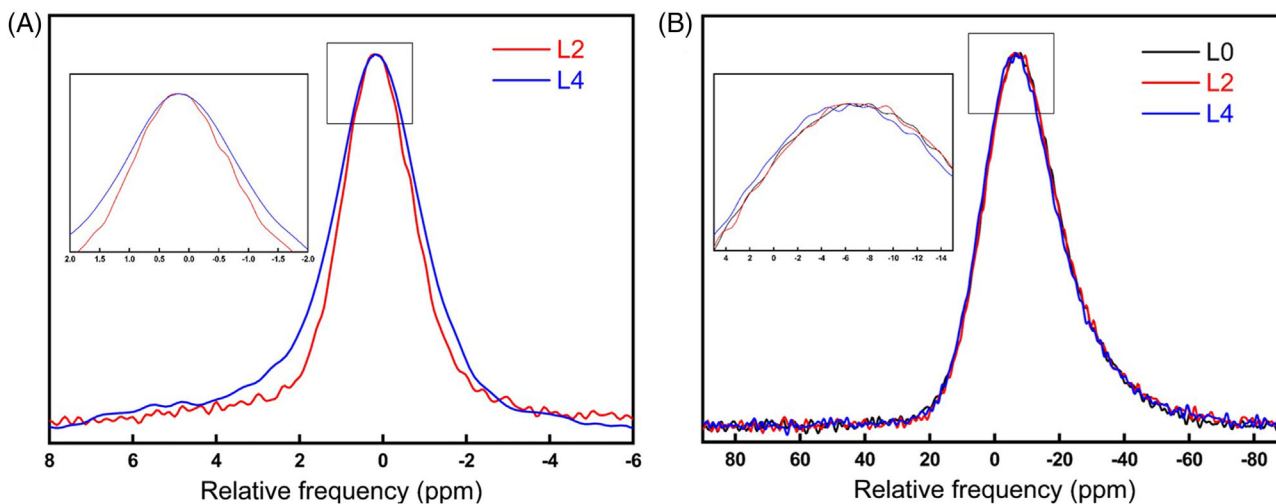


FIGURE 2 (A) ^7Li MAS NMR spectra; (B) ^{23}Na MAS NMR spectra of glass samples. Insets show magnified view of the peak position

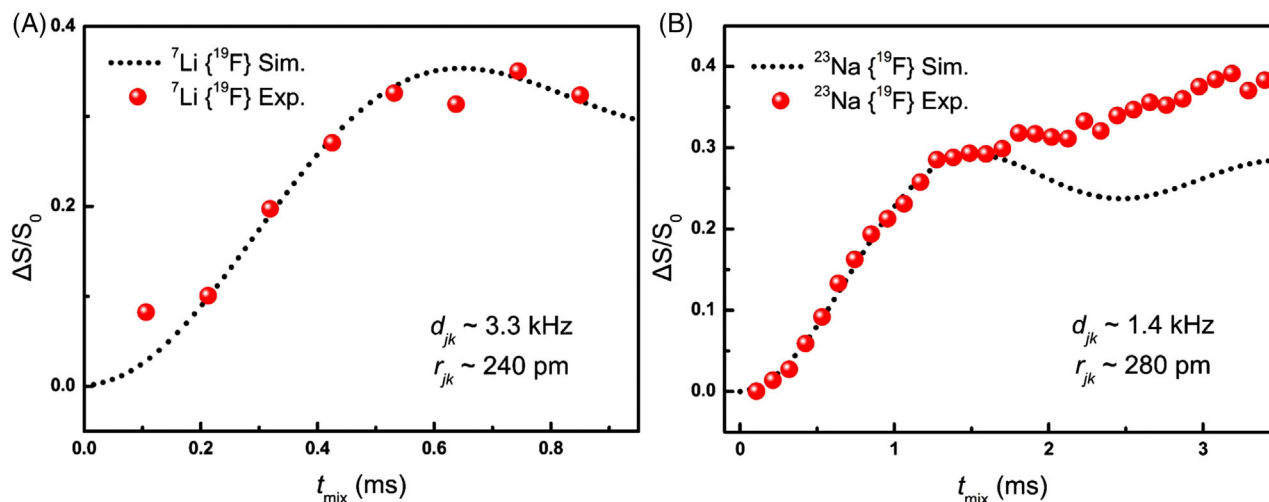


FIGURE 3 Experimental (circles) and simulated (dotted line) buildup curves assuming a spin-pair for (A) ${}^7\text{Li}\{{}^{19}\text{F}\}$ R³-REDOR NMR of L2 glass and (B) ${}^{23}\text{Na}\{{}^{19}\text{F}\}$ R³-REDOR NMR of L4 glass. The simulations are least-square fits of the data to Equation (2). The higher intensities for long t_{mix} in (B) are due to dipolar couplings from additional long-range ${}^{19}\text{F}$ spins

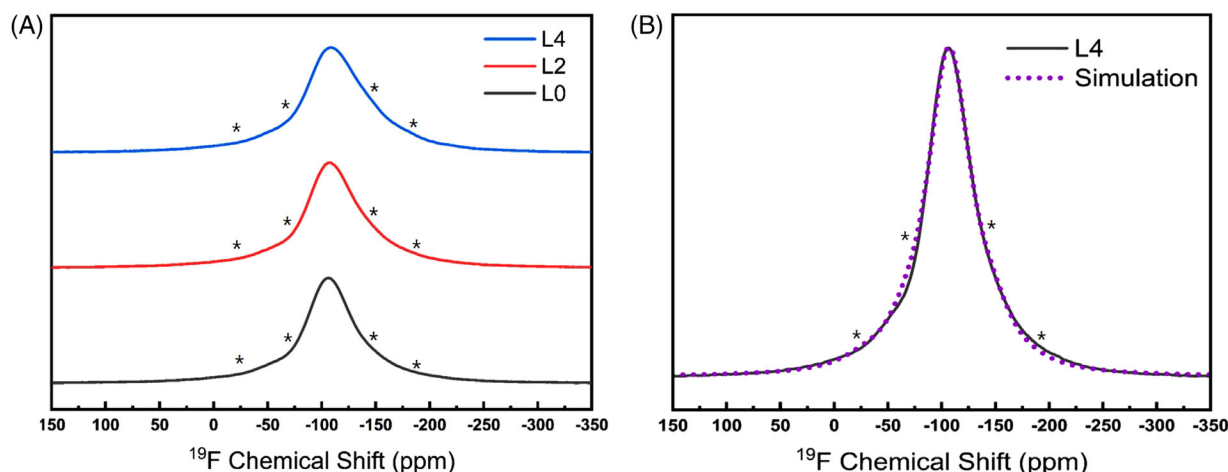


FIGURE 4 ${}^{19}\text{F}$ MAS NMR spectra of different glass samples. Asterisks denote location of spinning sidebands

structure. Similarly, the ${}^{23}\text{Na}\{{}^{19}\text{F}\}$ REDOR curve yields $d_{jk} \sim 1.4$ kHz, corresponding to a Na-F spin-pair distance of 2.8 Å (Figure 3B). This distance is again much longer than a typical Na-F bond of $\sim 1.9 \pm 0.1$ Å, indicating no direct bonding between sodium and fluorine in the glass structure. Therefore, the increased crystallization delay of cuspidine with progressive addition of Li_2O in these glasses cannot be ascribed to any bonding interactions between Li/Na and F in the network.

The ${}^{19}\text{F}$ MAS NMR spectra of all glasses appear to be rather similar with a single resonance centered near -106.9 ppm with some overlapping intensity from the spinning sidebands (Figure 4). This ${}^{19}\text{F}$ isotropic chemical shift is characteristic of $\text{F}-(\text{Ca})_n$ bonding environments in both CaF_2 (fluorite, -108.5 ppm) and cuspidine (-101.6

and -106.1 ppm),²⁹ but it is rather different from that characteristic of either crystalline LiF (-200 ppm) or NaF (-240 ppm).^{30,31} Therefore, in these glasses the F atoms are primarily bonded to Ca regardless of their Li contents.

The ${}^{29}\text{Si}$ MAS NMR spectra (Figure 5A) of these glasses show a broad resonance centered near $\delta_{\text{iso}} \sim -77$ ppm, consistent with the structure dominated by the presence of Q¹ units that is, $[\text{Si}_2\text{O}_7]^{-6}$ dimers. It may be noted that this δ_{iso} is rather similar to that (-79.9 ppm) characteristic of the Q¹ units in the structure of crystalline cuspidine.²⁹ As shown in Figure 5B, the ${}^{29}\text{Si}$ MAS NMR spectral line shapes of L0, L2, and L4 glass samples can be simulated well with three resonances centered at ~ -62 , -76 , and -90 ppm, corresponding to Q⁰, Q¹, and Q²

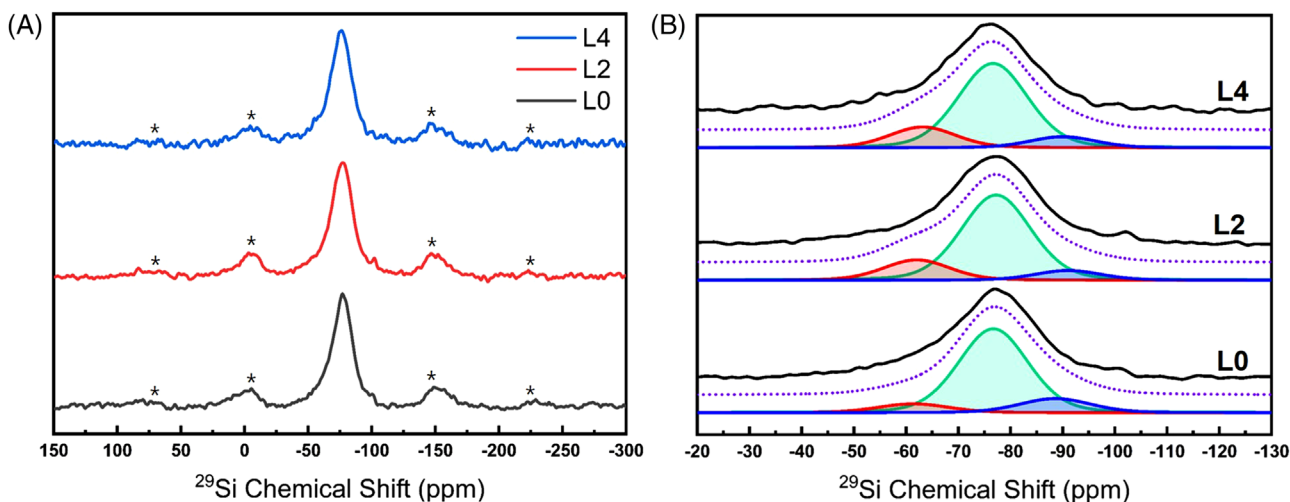


FIGURE 5 (A) ^{29}Si MAS NMR spectra of different glass samples. Asterisks denote spinning sidebands. (B) Experimental (solid black line) and simulated (dot violet line) ^{29}Si MAS NMR spectra of L0, L2, and L4 glass samples. Individual simulation components for Q^0 , Q^1 , and Q^2 units are denoted in red, green, and blue, respectively

TABLE 3 Parameters used for simulation of ^{29}Si NMR spectra of L0, L2, L4 glass samples in Figure 5B; peak position, width, and relative fractions of constituent Q species

	Peak position (± 2 ppm)			Width (± 3 ppm)			Relative fraction ($\pm 3\%$)		
	Q^0	Q^1	Q^2	Q^0	Q^1	Q^2	Q^0	Q^1	Q^2
L0	-61	-76	-89	15	15	15	8	78	14
L2	-62	-76	-90	15	15	15	14	75	11
L4	-62	-76	-90	15	15	15	15	75	10

units, respectively, and the relative fractions of these units can be obtained from the respective peak areas (Table 3). Here Q^n represents the standard nomenclature for SiO_4 tetrahedra with n bridging oxygen atoms. The number of non-bridging oxygen (NBO) atoms per SiO_4 tetrahedron (NBO/Si), calculated from the relative fractions of the constituent Q^n species yield NBO/Si ~ 3.02 and 3.10 , respectively, for L0 and L4 glass samples, which implies unusually high depolymerization states for silicate glasses. The higher NBO/Si of the L4 glass is consistent with the expectation that the addition of Li_2O depolymerizes the silicate network and consequently increases the NBO concentration.

When taken together, these multi-nuclear NMR data suggest that the structure of these glasses consist of $[\text{Si}_2\text{O}_7]^{-6}$ dimers. The NBOs on these dimers are bonded to Ca, Na, and Li modifier cations and form the coordination polyhedra of the latter. Additionally, the F atoms are exclusively bonded to Ca atoms in the structure. As the parent melts are cooled from above T_m , the Na and Li ions must move away to create locally Ca-rich regions with composition and structure similar to that of cuspidine, which results in the nucleation and crystallization of the latter near T_c . The increased undercooling required

for the crystallization of cuspidine upon addition of Li_2O is opposite to what has been reported for an increase in the Na_2O content in single-alkali glasses^{11,12} and clearly cannot be ascribed to the lowering in the thermodynamic activity of the cuspidine components owing to the formation of Li-F bonds or to the increase in the NBO:F ratio. We hypothesize that the increased undercooling due to the addition of Li_2O to the Na_2O -containing base composition originates from chemically frustrated local structure produced by multiple alkali ions, which increases the energy barrier to nucleation. This “mixed-alkali” effect should not be confused with the well-known slowdown of the motion of alkali ions that results from the coexistence of two different ions, which block each other’s diffusion pathways, as the latter effect weakens with increasing temperature above the glass transition and is likely to be non-existent at the temperature of crystallization of cuspidine from the melt.³²

Finally, the ^{11}B MAS NMR spectra of these glasses (Figure 6) are characterized by a broad quadrupolar line shape centered near ~ 14 ppm, which can be readily assigned to BO_3 units and a weak Gaussian resonance centered at ~ 0.9 ppm that corresponds to a small fraction of tetrahedral BO_4 units.³³ Simulation of these line shapes

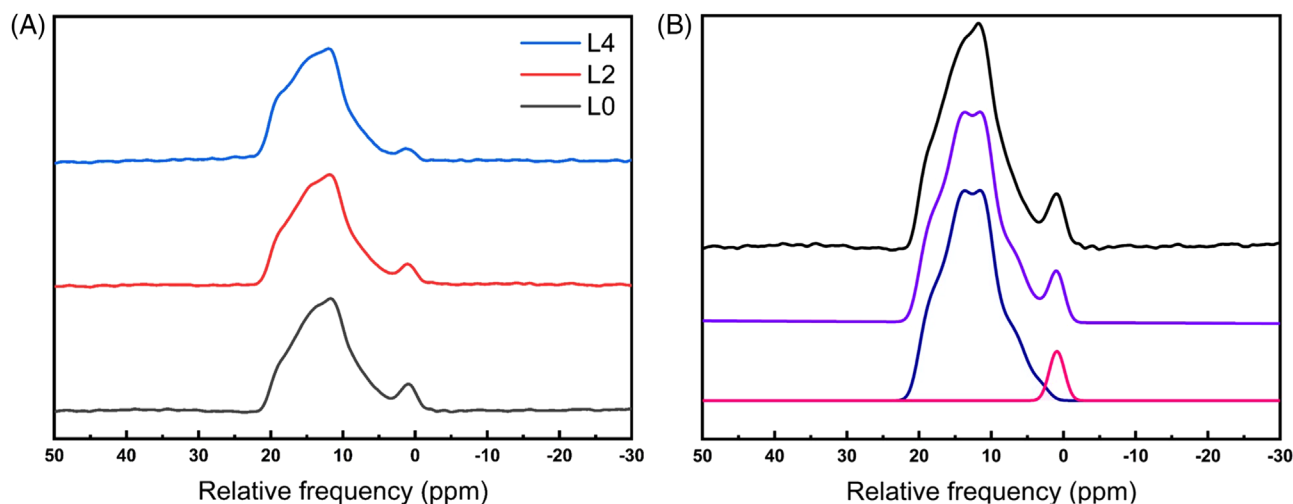


FIGURE 6 (A) Experimental ^{11}B MAS NMR spectra of L0, L2, and L4 glasses. (B) Experimental (top) and simulated (middle) ^{11}B MAS NMR spectra of L0 glass. Individual simulation components for BO_3 and BO_4 units are shown at the bottom

were carried out using the software Dmfit³⁴ (Figure 6B). The relative concentration of the BO_4 units in the structure of these glasses progressively decreases from $\sim 5\%$ to $\sim 2.5\%$ with increasing Li_2O content, which indicates the formation of NBOs on the B atoms with increasing modifier content. Simulation of the quadrupolar line shape yields an isotropic shift of 20.4 ppm, a quadrupolar coupling constant $C_Q = 2.6$ MHz and an asymmetry parameter η_Q for the electric field gradient of ~ 0.6 for the BO_3 environment. Previous high-resolution ^{11}B NMR studies of crystalline borates have shown that such a high value of η_Q is characteristic of BO_3 units in chain-like metaborate units, although dimeric pyroborate units can also display η_Q of up to 0.5.³³ Moreover, the isotropic shift of the BO_3 units suggest the absence of any B-O-Si linkages in these glasses.³⁵ Therefore, we argue that the formation of these metaborate chains frustrate crystallization by weaving through the glass structure and thereby stabilize these glasses against devitrification. If the B atoms predominantly form B-O-B linkages in metaborate units then each B atom will have 1 NBO and considering that each formula unit of CaO , Na_2O , and Li_2O as network modifiers contribute two NBOs, one obtains NBO/Si for the L0 and L4 glasses to be ~ 2.8 and 3.0, respectively. These estimates are indeed in good agreement with the NBO/Si values of ~ 2.94 and 3.05 for these two glasses derived from ^{29}Si MAS NMR line shape simulation (vide supra).

4 | CONCLUSION

The multi-nuclear single- and double- resonance NMR spectroscopic results indicate that the structure of highly modified $\text{CaO}-(\text{Na,Li})_2\text{O}-\text{SiO}_2-\text{CaF}_2$ mold flux glasses

consists of a network of modifier (Ca,Na,Li)-oxygen polyhedra that are sparsely cross-linked via Q^1 dimers. The corresponding melts form bulk glasses at laboratory cooling rates upon incorporation of ~ 4 mol% B_2O_3 , which prevents rapid crystallization of cuspidine via the formation of metaborate chains that intersperse through the glass structure. The exclusive bonding of F to Ca and the presence of $\text{Ca}(\text{O,F})_n$ coordination polyhedra linked via Q^1 dimers in the structure of these glasses imply that locally Ca-rich regions, if formed in the structure through diffusion of the alkali away from such regions, can act as precursors for the nucleation of cuspidine upon slow undercooling of the parent melts below their liquidus temperature. The degree of undercooling required for the crystallization of cuspidine progressively increases with increasing addition of Li to a Na-containing base composition. Such a trend is likely a manifestation of an increased chemical frustration of the local structure due to the mixing of alkalis.

ACKNOWLEDGMENTS

This research was supported by the Korea Institute for Advancement of Technology (KIAT) grant funded by the Korea Government (MOTIE) (P0017304, Human Resource Development Program for Industrial Innovation). The authors also greatly appreciate the financial support from POSCO Research Laboratory, Pohang, Korea. Also, this work was supported by the Industrial Strategic Technology Development Program (Grant number 10063056), funded by the Ministry of Trade, Industry & Energy (MOTIE), Korea. S.S. acknowledges support from an NSF grant (DMR-1855176) and from the Blacutt-Underwood Professorship at UC Davis. The National High Magnetic Field Laboratory (NHMFL) in Tallahassee, FL, USA, is supported by NSF DMR-1644779 and the State of Florida.

ORCID

Tae-min Yeo  <https://orcid.org/0000-0002-1031-7090>Jung-Wook Cho  <https://orcid.org/0000-0003-2364-1938>Sabyasachi Sen  <https://orcid.org/0000-0002-4504-3632>

REFERENCES

- Cho J, Shibata H, Emi T, Suzuki M. Radiative heat transfer through mold flux film during initial solidification in continuous casting of steel. *ISIJ Int.* 1998;38(3):268–75.
- Cho JW, Emi T, Shibata H, Suzuki M. Heat transfer across mold flux film in mold during initial solidification in continuous casting of steel. *ISIJ Int.* 1998;38(8):834–42.
- Yeo T-m, Cho J-W, Alloni M, Casagrande S, Carli R. Structure and its effect on viscosity of fluorine-free mold flux: substituting CaF₂ with B₂O₃ and Na₂O. *J Non-Cryst Solids.* 2020 Feb 1;529:119756.
- Watanabe T, Hashimoto H, Hayashi M, Nagata K. Effect of alkali oxides on crystallization in CaO–SiO₂–CaF₂ glasses. *ISIJ Int.* 2008;48(7):925–33.
- Zhou L, Wang W, Ma F, Li J, Wei J, Matsuura H, et al. A kinetic study of the effect of basicity on the mold fluxes crystallization. *Metall Mater Trans B.* 2012;43(2):354–62.
- Lu B, Wang W, Li J, Zhao H, Huang D. Effects of basicity and B₂O₃ on the crystallization and heat transfer behaviors of low fluorine mold flux for casting medium carbon steels. *Metall Mater Trans B.* 2013;44(2):365–77.
- HG R, ZT Z, JW C, GH W, Sridhar S. Crystallization behaviors of slags through a heat flux simulator. *ISIJ Int.* 2010 Aug;50(8):1142–50.
- Harada Y, Sakaguchi S, Mizoguchi T, Saito N, Nakashima K. Shear rate and crystalline phase effects on the super-cooling degree and crystallization behavior of CaO–SiO₂–CaF₂–RO (R = Mg, or Sr) flux systems. *ISIJ Int.* 2017 Aug;57(8):1313–8.
- Yang J, Zhang J, Sasaki Y, Ostrovski O, Zhang C, Cai D, et al. In-situ study of crystallisation behaviour of CaO–SiO₂–Na₂O–B₂O₃–TiO₂–Al₂O₃–MgO–Li₂O fluorine-free mould fluxes with different CaO/SiO₂ ratios. *ISIJ Int.* 2016 Apr;56(4):574–83.
- Wang W, Yan X, Zhou L, Xie S, Huang D. Influences of basicity and Li₂O on the properties of fluorine-free mold flux for the casting of medium carbon steels. *Metall Mater Trans B.* 2016 Apr;47(2):963–73.
- Li J, Wang W, Wei J, Huang D, Matsuura H. A kinetic study of the effect of Na₂O on the crystallization behavior of mold fluxes for casting medium carbon steel. *ISIJ Int.* 2012 Dec;52(12):2220–5.
- Wei J, Wang W, Zhou L, Huang D, Zhao H, Ma F. Effect of Na₂O and B₂O₃ on the crystallization behavior of low fluorine mold fluxes for casting medium carbon steels. *Metall Mater Trans B.* 2014;45(2):643–52.
- Seo M-D, Shi C-B, Cho J-W, Kim S-H. Crystallization behaviors of CaO–SiO₂–Al₂O₃–Na₂O–CaF₂–(Li₂O–B₂O₃) mold fluxes. *Metall Mater Trans B.* 2014 Oct;45(5):1874–86.
- Lee J-h, Yeo T-m, Cho J-W. Effect of Li₂O on melt crystallization of CaO–SiO₂–CaF₂ based glasses. *Ceram Int.* 2021 Mar 1;47(5):6773–8.
- Yeo T-m, Jeon J-M, Hyun S-H, Ha H-M, Cho J-W. Effects of Li₂O on structure of CaO–SiO₂–CaF₂–Na₂O glasses and origin of crystallization delay. *J Mol Liq.* 2022 Feb 1;347:117997.
- Allibert M, Gaye H, Geiseler J, Janke D, Keene BJ, Kirner D, et al. *SLAG ATLAS*, 2nd edn. Düsseldorf: Verlag Stahleisen GmbH; 1995.
- Uchino T, Yoko T. Sodium and lithium environments in single- and mixed-alkali silicate glasses. An ab Initio molecular orbital study. *J Phys Chem B.* 1999;103(11):1854–8.
- Saburi S, Kawahara A, Henmi C, Kusachi I, Kihara K. The refinement of the crystal structure of cuspidine. *Mineral. J.* 1977;8(5):286–98.
- Joubert O, Magrez A, Chesnaud A, Caldes MT, Jayaraman V, Piffard Y, et al. Structural and transport properties of a new class of oxide ion conductors: Nd₄ [Ga₂ (1–x)M₂xO₇+ x□ 1– x] O₂ (M = Ti, Ge). *Solid State Sci.* 2002 Nov;4(11–12):1413–8.
- Park JH, Min DJ, Song HS. FT-IR spectroscopic study on structure of CaO–SiO₂ and CaO–SiO₂–CaF₂ slags. *ISIJ Int.* 2002 Jan;42(4):344–51.
- Nagata K, Fukuyama H. Physicochemical properties of CaO–SiO₂–CaF₂–NaF slag system as a mold flux of continuous casting. *Steel Res Int.* 2003 Jan;74(1):31–5.
- Gan Z. Rotary resonance echo double resonance for measuring heteronuclear dipolar coupling under MAS. *J Magn Reson.* 2006 Dec;183(2):235–41.
- Gullion T. Rotational-echo, double-resonance NMR. In: Webb GA, ed. *Modern Magnetic Resonance*. Springer; 2008. p. 713–8.
- Mueller K, Jarvie T, Aurentz D, Roberts B. The REDOR transform: direct calculation of internuclear couplings from dipolar-dephasing NMR data. *Chem Phys Lett.* 1995 Sep 1;242(6):535–42.
- Harris RK, Becker ED, De Menezes SMC, Goodfellow R, Granger P. NMR nomenclature: nuclear spin properties and conventions for chemical shifts (IUPAC Recommendations 2001). *Pure Appl Chem.* 2001;73(11):1795–818.
- Yeo T-m, Cho J-W. Effect of Li₂O on non-isothermal crystallization of cuspidine in CaO–SiO₂–CaF₂ glasses. *Metall Mater Trans B.* 2021 May 4;52(4):2186–93.
- Youngman R. NMR spectroscopy in glass science: a review of the elements. *Materials.* 2018 Mar 22;11(4):476.
- Xue X, Stebbins JF. ²³Na NMR chemical shifts and local Na coordination environments in silicate crystals, melts and glasses. *Phys Chem Miner.* 1993 Oct;20(5):297–307.
- Hansen MR, Jakobsen HJ, Skibsted J. ²⁹Si chemical shift anisotropies in calcium silicates from high-field ²⁹Si MAS NMR spectroscopy. *Inorg Chem.* 2003 May;42(7):2368–77.
- Jain P, Kim S, Youngman RE, Sen S. Direct observation of defect dynamics in nanocrystalline CaF₂: results from ¹⁹F MAS NMR spectroscopy. *The Journal of Physical Chemistry Letters.* 2010 Mar;1(7):1126–9.
- Sadoc A, Body M, Legein C, Biswal M, Fayon F, Rocquefelte X, et al. NMR parameters in alkali, alkaline earth and rare earth fluorides from first principle calculations. *Phys Chem Chem Phys.* 2011 Nov 7;13(41):18539–50.
- Day DE. Mixed alkali glasses—their properties and uses. *J Non-Cryst Solids.* 1976 Aug;21(3):343–72.
- Kroeker S, Stebbins JF. Three-coordinated boron-II chemical shifts in borates. *Inorg Chem.* 2001 Nov 19;40(24):6239–46.
- Massiot D, Fayon F, Capron M, King I, Le Calvé S, Alonso B, et al. Modelling one- and two-dimensional solid-state NMR spectra. *Magn Reson Chem.* 2002 Jan;40(1):70–6.

35. Martens R, Müller-Warmuth W. Structural groups and their mixing in borosilicate glasses of various compositions—an NMR study. *J Non-Cryst Solids*. 2000 Mar 2;265(1-2):167–75.

SUPPORTING INFORMATION

Additional supporting information can be found online in the Supporting Information section at the end of this article.

How to cite this article: Yeo T-m, Cho J-W, Hung I, Gan Z, Sen S. Structure and crystallization behavior of complex mold flux glasses in the system CaO-Na₂O-Li₂O-CaF₂-B₂O₃-SiO₂: A multi-nuclear NMR spectroscopic study. *J Am Ceram Soc*. 2022;105:6140–6148.
<https://doi.org/10.1111/jace.18610>